frontiers in Veterinary Science

TYPE Original Research
PUBLISHED 12 June 2026
DOI 10.3389/fvets.2026.1834730

OPEN ACCESS

EDITED BY
Jianzhu Liu,
Shandong Agricultural University, China

REVIEWED BY
Ni Made Puspawati,
Udayana University, Indonesia
Cristian dos Santos Pereira,
Federal University of Pará, Brazil

*CORRESPONDENCE
Giulia Biondolillo
giulia.biondolillo2@unibo.it

†PRESENT ADDRESS
Luca Melotti,
Department of Human Sciences,
Link Campus University, Rome, Italy

‡These authors have contributed equally to this work and share first authorship

RECEIVED 19 March 2026
REVISED 21 May 2026
ACCEPTED 25 May 2026
PUBLISHED 12 June 2026

CITATION
Antognoni F, Tubon I, Biondolillo G, Melotti L, Di Lecce R, Afifi SM, Salaroli R, Vaca G, Gomez CV, Cárdenas GOZ, Forni M, Zannoni A and Bernardini C (2026) Microencapsulated *Vaccinium floribundum* Kunth extract promotes endothelial angiogenesis *in vitro* and attenuates inflammation *in vitro* and *in vivo*. *Front. Vet. Sci.* 13:1834730. doi: 10.3389/fvets.2026.1834730

Microencapsulated *Vaccinium floribundum* Kunth extract promotes endothelial angiogenesis *in vitro* and attenuates inflammation *in vitro* and *in vivo*

Fabiana Antognoni[1‡], Irvin Tubon[2‡], Giulia Biondolillo[3*], Luca Melotti[4†], Roberta Di Lecce[1], Sherif M. Afifi[1], Roberta Salaroli[3], Gabriela Vaca[5], Cristian Vacacela Gomez[6], Goering Octavio Zambrano Cárdenas[7], Monica Forni[8,9], Augusta Zannoni[3,9] and Chiara Bernardini[3,9]

[1]Department for Life Quality Studies, University of Bologna, Rimini, Italy, [2]Facultad de Salud Pública, Escuela Superior Politécnica de Chimborazo, Riobamba, Ecuador, [3]Department of Veterinary Medical Sciences, University of Bologna, Bologna, Italy, [4]Department of Comparative Biomedicine and Food Science, University of Padua, Padua, Italy, [5]Facultad de Ciencias Médicas, Universidad Regional Autónoma de los Andes (UNIANDES), Ambato, Ecuador, [6]Universidad Ecotec, Samborondón, Ecuador, [7]Carrera de Ingeniera Ambiental, Sede Morona Santiago, Escuela Superior Politécnica de Chimborazo, Macas, Ecuador, [8]Department of Medical and Surgical Sciences, University of Bologna, Bologna, Italy, [9]Health Sciences and Technologies-Interdepartmental Center for Industrial Research (CIRI-SDV), Alma Mater Studiorum-University of Bologna, Bologna, Italy

Introduction: Natural products, especially polyphenol-rich medicinal plants, are increasingly investigated as multitarget therapeutics in both human and veterinary medicine for angiogenic regenerative properties and for inflammation based-diseases. Recent developments in natural product formulation, notably microencapsulation, have been shown to improve stability, bioavailability, and controlled release of bioactive compounds. The integration of complementary *in vitro* and *in vivo* models is critical for evaluating both efficacy and preliminary bioactivity for assessing the translational potential.

Methods: In the present study assessed the phytochemical composition and biological activity of a microencapsulated Ecuadorian *Vaccinium floribundum* extract (VFM), using a combination of *in vitro* and *in vivo* approaches.

Results and Discussion: VFM chemical characterization identified 17 compounds belonging to different classes, including anthocyaninin, flavonoids, procyanidins, dihydrochalcones, and phenolic acids. Chlorogenic acid and quercetin were the most abundant metabolites, and cyanidine-3-*O*-galactoside and petunidin-3-*O*-glucoside were the main anthocyanins detected, confirming a rich bioactive profile. Primary porcine thoracic aortic endothelial cells (pAEC) were treated with VFM to assess cell viability and angiogenic potential and challenged with bacterial lipopolysaccharide (LPS) in the presence or absence of the extract. Anti-inflammatory effects were further evaluated in vivo using a carrageenan-induced mouse paw edema model. VFM enhanced endothelial cell viability, promoted capillary-like networks, and modulated early angiogenic signaling pathways; moreover it mitigated LPS-induced endothelial dysfunction by reducing pro-inflammatory markers (cytokines, inducible Nitric Oxide Synthase - iNOS, Vascular Cell Adhesion Molecule 1 - VCAM-1). *in vivo*, paw edema assays

demonstrated that VFM exhibited anti-inflammatory activity under the tested conditions. These findings support the traditional use of *Vaccinium floribundum* and highlight its potential for developing nutraceutical formulations targeting vascular and inflammatory disorders.

KEYWORDS

angiogenesis, anthocyanins, Ecuadorian flora, endothelial cells, *in vitro*/*in vivo* animal model, inflammation, phytoextract, polyphenols

1 Introduction

In recent decades, there has been a substantial increase in scientific interest in natural products as therapeutic agents for both human and veterinary health. This trend is driven by the need to identify more safe and effective alternatives to synthetic drugs, particularly in the context of chronic and multifactorial diseases. Among natural source, medicinal plants have attracted particular attention due to their richness in bioactive metabolites, including phenolic compounds, flavonoids and terpenoids (1). These secondary metabolites are capable of modulating multiple molecular targets simultaneously. Such multitarget activity is especially relevant in complex biological processes that require fine regulatory balance.

Inflammation and angiogenesis are closely interconnected biological processes that operate in a coordinated manner to regulate tissue homeostasis, repair, and adaptation to injury (2, 3). Beyond their established roles in physiological contexts such as wound healing and embryonic development, the sustained activation of inflammatory and angiogenic pathways represents a hallmark of numerous pathological conditions, including chronic inflammatory diseases, cancer, and autoimmune disorders among others (4). Due to inflammation process occurring at both local and systemic levels, the integrated application of *in vitro* and *in vivo* models is essential for its comprehensive characterization. *In vitro* systems enable the detailed research of cellular responses and molecular signalling pathways under tightly controlled experimental conditions, whereas *in vivo* models recreate the complexity of the whole organism by incorporating systemic interactions and physiologically relevant immune dynamics. The complementary use of these approaches strengthens mechanistic interpretation and improves the translational assessment of potential therapeutic agents. Animal models have been fundamental for investigating normal physiology, understanding disease pathophysiology, and testing the safety and efficacy of new therapies in preclinical studies. This widespread usage is attributed to the genetic similarities between humans and various mammal species (5). Various studies have used different models to investigate inflammatory responses, highlighting the use of animals, especially rodents, to recreate acute inflammatory conditions. Moreover, these preclinical models not only facilitate the elucidation of underlying immunopathological mechanisms but also evaluate the pharmacodynamic efficacy and safety profiles of candidate anti-inflammatory agents (6). In this context, experimental models of acute inflammation are essential for understanding the underlying mechanisms and exploring potential therapeutic interventions. Large animal models play a crucial complementary role to small rodents by offering closer anatomical (7), physiological, and immunological similarity to humans. Among them, the pig model is particularly valuable in inflammation and angiogenesis research due to its comparable cardiovascular system, skin structure, wound healing response, and immune repertoire. Porcine models are widely used to study ischemia-induced angiogenesis, chronic inflammatory diseases, and biomaterial–tissue interactions. Among *in vitro* studies using the pig model, primary porcine Aortic Endothelial Cell cultures (pAEC) exhibit well-characterized morphological and molecular changes upon exposure to the pro-inflammatory lipopolysaccharide (LPS), including modulation of nitric oxide synthase expression, alteration of cell morphology, and induction of inflammatory signalling cascades, which closely mirror features of endotoxin-induced endothelial dysfunction observed *in vivo*. Importantly, this *in vitro* cell platform supports the evaluation of phytochemicals as protective agents against LPS-mediated damage, providing a controlled and reproducible experimental setting to assess their ability to preserve endothelial integrity and functionality under inflammatory conditions. The use of pAEC allows for the systematic investigation of plant-derived compounds in terms of their overall cytoprotective and anti-inflammatory potential, thereby offering valuable preliminary insights into their suitability for modulating endothelial responses to inflammatory insults (8–11).

Vaccinium floribundum Kunth is a wild berry species of Ericaceae family growing in Ecuador's Andean highlands, commonly known as mortiño (12). It is a semi-evergreen shrub, reaching 1.5 m in height, with lanceolate leaves that produce round, bluish-black berries with a pleasant flavour, mostly consumed in the local culinary tradition in jams, wine, and boiled drinks. Like most blueberries and cranberries, mortiño fruits are currently considered as "superfruits," thanks to their high concentration of bioactive compounds mainly belonging to the class of phenolics, including polyphenols, flavonoids, anthocyanins, and proanthocyanidins, and their well-recognized health-beneficial effects including antioxidant, antinflammatory, and antimicrobial ones (13, 14). Therefore, it is crucial to ensure that bioactive compounds remain unchanged from their production until their consumption; in this context, microencapsulation is currently regarded as one of the most widely used strategies to preserve their stability and bioactivity, thereby enhancing the efficacy and applicability of these extracts *in vivo* and *in vitro* trials (15). In this work the phytochemical composition and the biological potential of a microencapsulated extract of *Vaccinium floribundum* berries was evaluated, with the aim of providing a scientific support to the anti-inflammatory and the angiogenic properties of this plant, using *in vitro* and *in vivo* models.

2 Materials and methods

2.1 Chemical and reagents

Cell culture plates and glass slides were obtained from Corning Life Sciences (NC 27712 USA). Human Endothelial Serum-Free

Medium (hESFM), heat-inactivated fetal bovine serum (FBS), antibiotic-antimycotic, Dulbecco's phosphate-buffered saline (DPBS), phosphate-buffered saline (PBS), and Geltrex™ LDEV-Free Reduced Growth Factor Basement Membrane Matrix were purchased from Gibco-Life Technologies (Carlsbad CA, USA). Trypsin–EDTA solution 1X, Dimethyl sulphoxide (DMSO), lipopolysaccharide (LPS) (*E. coli* 055: B5), *In vitro* Toxicology Assay Kit and Cell Growth Determination Kit MTT based and Maltodextrin (DE 10–20) was used as wall material for microencapsulation were purchased from Merck- Sigma-Aldrich (St. Louis, MO, USA). TRIzol reagent was purchased from Thermo Fisher Scientific (Waltham, MA, USA). RNA isolation was performed with a NucleoSpin RNA II kit (MACHEREY NAGEL GmbH & Co. KG, Düren, Germany), and an iScript cDNA Synthesis Kit and iTaq Universal SYBR Green Supermix were used for cDNA synthesis and qPCR analysis, respectively (Bio-Rad Laboratories Inc., Hercules, CA, USA). A commercial porcine IL-8 sandwich ELISA kit (Elabscience, TX, USA; Cat. No. E-EL-P3004) was used for cytokine quantification. The absence of mycoplasma contamination was periodically verified using the EZ-PCR Mycoplasma Detection Kit (Biological Industries, Kibbutz Beit-Haemek, Israel). Chemical standards (chlorogenic, caffeic, *p*-coumaric, ferulic, protocatechuic acid, quercetin, quercetin-3-*O*-galactoside, quercetin-3-*O*-glucoside, quercetin-3-*O*-rhamnoside, quercetin-3-*O*-rutinoside, kaempferol, kaempferol-7-*O*-glucoside, cyanidin-3-*O*-galactoside chloride, catechin, epicatechin, procyanidin B1, procyanidin B2, procyanidin C1, phloretin, and phlorizin), all >95% pure, were purchased from Extrasynthese (Genay Cedex, France). Stock solutions of the analytes were prepared at 1 mg/mL in MeOH and stored at −20 °C until use. Working standard solutions were prepared daily from stock solutions by dilution with the corresponding mobile phase in its initial composition for phenolic acid and flavonoid analysis, respectively. HPLC-grade methanol (MeOH), acetronitrile, and water, formic acid, fluorescein, K_2HPO_4, 2,2′-azobis(2-amidinopropane) dihydrochloride (AAPH), 2,2-diphenyl-1-picrylhydrazyl (DPPH), and Trolox (Tx), all pure for analysis, were purchased from Merck Reagents (Milan, Italy).

2.2 Collection of plant material

The fruits of *Vaccinium floribundum* Kunth (mortiño), were collected, after obtaining authorization for non-commercial collection from the Ministry of Environment, Water and Ecological Transition (No. MAATE-ARSFC-2022-2801), in the province of Tungurahua, specifically in the parish of Pilahuín, at a latitude (Y): −78.7277812; longitude (X): −1.299677 and altitude: 3,054 meters above sea level. This process was carried out using simple random sampling to ensure the quality of the samples collected. The fruits were collected when they were in good condition, without damage from insects, animals, or environmental factors such as rain, sun, or wind. The plant material was identified by the herbarium of the Escuela Superior Politécnica de Chimborazo (No-ESPOCH-HERB-035) and immediately sterilized.

2.3 Preparation of plant material

Sodium hypochlorite solution at 9% was used to disinfect the fruits and subsequentially washed with abundant water to eliminate excess chlorine. Then a convection dehydrator (Memmert, USA) was used to dry the material at 40 °C for 48 to 72 h. Finally, the dried material was crushed using a blender until fine powder was obtained and stored in ziplock bags (15).

2.4 Extract preparation

The maceration method was used to obtain ethanolic extract from dry and crushed fruits. Thus, dried fruits with 50:50 ethanol: water ratio were placed in a glass container with a 1:10 ratio (w/v) and left to stand in the absence of light for 8 days, shaking occasionally to distribute the plant material in the solvent. After this time, the product was filtered, and the solvent was removed by rotary vacuum evaporation (Bucchi, Switzerland). Finally, the mortiño ethanolic fruit extract (VFE) was stored in sterile plastic tubes under refrigeration at 4 °C until use (16).

2.5 Microencapsulation process

The microencapsulation of plants extracts was performed using maltodextrin (10–20 DE) as the carrier agent. Extracts with a total solids content of 30% (equivalent to 20 g solids) were prepared at a 20:80 solid extract-to-maltodextrin ratio. For each extract, 280 mL of distilled water was mixed with the anthocyanin solution and combined with maltodextrin. The microencapsulation process using a laboratory-scale mini spray dryer Büchi B-290 (Flawil, St. Gallen, Switzerland). The solutions were fed into the spray dryer under controlled conditions: an inlet air temperature of 140 °C ± 2 °C, an outlet air temperature of 80 °C ± 2 °C, an internal pressure of −50 mbar, an atomizing air flow of 400–600 L/h, and a drying air flow rate of 60 m^3/h. During the spray drying process, each solution was atomized within the drying chamber, forming solid microspheres encapsulated in maltodextrin-based polymers. The resulting microspheres of the mortiño ethanolic fruit extract microencapsulated (VFM) were collected and stored in HDPE-aluminum bags at room temperature of 15 °C–25 °C (17).

2.6 Spray drying process yield and characterization by FTIR

Encapsulation yield after spray drying was calculated as a percentage as a ratio between the total microcapsule's powders weight and the weight of the carrier agents using the following equation:

$$Encapsulation\ Yield\ (\%) = \frac{weight\ (g)\ of\ the\ powder\ collected}{weight\ (g)\ of\ the\ carrier\ agents} \times 100$$

Fourier transform infrared (FTIR) spectroscopy was employed to identify the functional groups in the microcapsules. The spectra were obtained using a Perkin Elmer Spectrum two FTIR L1600312 spectrometer (Perkin Elmer, Tokyo, Japan) with the ATR method, covering a wave number range of 4,000–500 cm^{-1} at a resolution of 4 cm^{-1} across 36 scans (18).

2.7 HPLC-DAD analysis of phenolic acids and flavonoids in VFM

The identification and quantification of phenolic acids was performed according to Mattila and Kumpulainen (19) with modifications (20), using a Jasco (Tokyo, Japan) HPLC-DAD 4000 series system composed of a PU-4180 pump, an MD-4015 photodiode array detector, a XX oven and an AS-4050 autosampler. The stationary phase was an Agilent (Santa Clara, CS, USA) Zorbax Eclipse Plus C18 reverse-phase

column (4.6 × 100 mm, 3.5 μm) equipped with a Zorbax Eclipse Plus C18 precolumn. The mobile phase was composed by 4.5% of formic acid (FA, solution A) and acetonitrile (ACN, solution B) and the elution was carried out at a flow rate of 0.7 mL/min and a temperature of 24 °C, as follows: isocratic elution 97% A, 0–6 min; linear gradient from 97% A to 85% A, 6–17 min; linear gradient from 85% A to 82.8% A; 17–27 min; linear gradient from 82.8% A to 50% A, 27–40 min; linear gradient from 50% A to 97% A, 40–43 min; isocratic elution 97% A, 43–50 min. The injection volume for both standards and samples was 20 μL and analyte detection was performed by monitoring at 329, 287, 280, and 254 nm. Quantifications were carried out using pure standards and building calibration curves in the 0.3–80 ppm range for all considered analytes. The identification and quantification of flavonoids was performed according to the method by Wojdyło et al. (21) with modifications (9), using the same chromatographic system and column as described above. The mobile phase was composed by 50 mM phosphoric acid, pH 2.5 (solution A) and acetonitrile (solution B) and the elution was carried out at a flow rate of 0.5 mL/min and a temperature of 24 °C as follows: isocratic elution 97% A, 0–1 min; linear gradient from 97%A to 60%A, 1–31 min; linear gradient from 60% A to 36% A; 31–35 min; linear gradient from 36% A to 97% A, 35–37 min; isocratic elution 97% A, 37–47 min. The injection volume for both standards and samples was 20 μL and analyte detection was performed by monitoring at 360 and 280 nm. Quantifications were performed using pure standards and building a calibration curve in the range 0.3–80 ppm for all considered analytes.

2.8 HPLC–MS analysis of anthocyanins in VFM

The chromatographic system was an Agilent 1,260 Infinity coupled to Agilent Ultivo 6465B triple quadrupole LC–MS (Agilent Technologies Inc., Santa Clara, California, USA). The chromatographic separations were achieved by a Zorbax SB-C18 (4.6 × 150 mm, 3.5 μm) using a mobile phase composed of 0.1% FA in ACN (Component A) and 0.1% FA in water (Component B) flowing at 0.40 mL/min. The gradient elution program was optimized as below: 0 min, 5% A; 3 min, 10% B; 35 min, 11% B; 40 min, 20% B; 50 min, 30% B; 55 min, 5% B and held constant for 5 additional minutes for column reconditioning. The injection volume was 10 μL and injections were carried out through the autosampler integrated into the Agilent system.

The data were carried out in multiple reaction monitoring (MRM) scan mode, using electrospray ionization source in positive mode. The main parameters for the mass spectrometer were as follows: capillary voltage: 4.0 kV; gas temperature: 300 °C; gas flow: 13 L/min; nebuliser: 30 psi; sheath gas temperature: 300 °C; sheath gas flow: 10 L/min. The specific, analyte-dependent parameters are detailed in Table 1.

2.9 *In vitro* antioxidant activity assays

The *in vitro* antioxidant capacity of the microencapsulated extract was evaluated through the DPPH (2,2-diphenyl-1-picrylhydrazide) and the *Oxygen Radical Absorbance Capacity* (ORAC) assays as previously described (8).

2.10 Cell culture and treatment

Primary porcine aortic endothelial cells (pAEC) were isolated, expanded, and characterized as previously described (22). After isolation and expansion, cells were cryopreserved until further required. For experimental procedures, pAEC were seeded and routinely cultured in T25 or T75 flasks (2×10^4 cells/cm^2) in Human Endothelial Serum-Free Medium (hESFM) supplemented with 5% Fetal Bovine Serum (FBS) and 1% antibiotic–antimycotic solution. Cells were maintained at 38.5 °C in a humidified atmosphere containing 5% CO_2. Cell cultures were routinely checked for mycoplasma contamination. At approximately 70%–80% confluence, cells were exposed to the experimental treatments.

VFM extract was tested at increasing concentrations (1 ng/mL, 10 ng/mL, 100 ng/mL, 1 μg/mL, 10 μg/mL, 100 μg/mL, and 1 mg/mL) for cell viability assessment. Based on viability results, selected concentrations of VFM (0.1 and 1 mg/mL) were used for subsequent experiments, either alone or in combination with lipopolysaccharide (LPS; 10 μg/mL). For gene expression analyses (qPCR), confluent pAEC (approximately 1×10^5 cells/well) were treated with the highest and most effective concentration based on viability test of VFM (1 mg/mL) in the absence or presence of LPS (25 μg/mL) for 5 h.

For the capillary-like tube formation assay, cells were seeded onto GelTrex™ -coated chambers and exposed to VFM (0.1 or 1 mg/mL), and tube formation was evaluated after 5 h.

Untreated cells cultured under identical conditions served as controls in all experiments.

2.11 Cell viability

Cell viability was evaluated using an MTT-based assay. Briefly: sixth-passage pAEC were seeded in 96-well culture plates at a density of 2×10^4 cells/well and incubated for 24 h. Afterwards, the culture medium was then replaced with hESFM supplemented with 5% FBS containing increasing concentrations of VFM or LPS, alone or in combination and cells were incubated for an additional 24 h at 38.5 °C and 5% CO_2.

After treatment, cells were incubated with MTT solution (0.5 mg/mL) for 3 h at 38.5 °C and 5% CO_2. Subsequently, 0.1 mL of MTT solubilisation solution was added to each well to dissolve the formazan crystals.

TABLE 1 Optimised MRM MS parameters.

Compound	Ion mode	Precursor ion (*m/z*)	Product ion (*m/z*)	Collision energy (V)
Cyanidin-3-*O*-galactoside	+	449	287	25
Petunidin-3-*O*-glucoside	+	479	317	25
Peonidin-3-*O*-glucoside	+	463	301	25
Delphinidin	+	303	229	40
Cyanidin	+	287	213	40

Absorbance was measured at 570 nm using Infinite® F50/ Robotic microplate reader (TECAN Life Sciences, Männedorf, Switzerland). For blank subtraction wells with only medium were used.

2.12 Quantitative real time PCR

RNA extraction was performed from pAECs seeded in a 24-well plate exposed to VFM (1 mg/mL) alone or in combination with LPS (25 μg/mL), for 5 h or 24 h by using the TRIzol reagent and NucleoSpin RNA II kit, according to the manufacturer's instructions.

After medium removal, 500 μL of TRIzol reagent were added to each well, and cells were lysed for 3 min at room temperature. Lysates were transferred into microcentrifuge tubes, mixed with 200 μL of chloroform, incubated for 10 min, and centrifuged (12,000×*g* for 15 min). The aqueous phase was recovered, mixed with an equal volume of 70% ethanol, and the resulting solution was applied to the NucleoSpin RNA Column for purification.

After spectrophotometric quantification, total RNA (250 ng) was reverse-transcribed into cDNA using the iScript cDNA Synthesis Kit (Bio- Rad) in a final volume of 20 μL.

All amplification reactions were performed in 20 μL and analyzed in duplicates (10 μL/well). The multiplex PCR contained the following: 10 μL of iTaqMan Probes Supermix (Bio-Rad), 1 μL of forward and reverse primers (5 μM each) of each reference gene, 0.8 μL of iTaqMan probes (5 μM) of each reference gene, 2 μL of cDNA, and 2.6 μL of water. The following temperature profiling was used: initial denaturation at 95 °C for 30 s followed by 40 cycles of 95 °C for 5 s and 60 °C for 30 s. The SYBR Green reaction contained the following: 10 μL of iQ SYBR Green Supermix (Bio-Rad), 0.8 μL of forward and reverse primers (5 μM each) for each target gene, 2 μL of cDNA, and 7.2 μL of water. The real-time program included an initial denaturation period of 1.5 min at 95 °C, 40 cycles at 95 °C for 15 s, and 60 °C for 30 s, followed by a melting step with ramping from 55 °C to 95 °C at a rate of 0.5 °C/10 s. To evaluate gene expression profiles, quantitative real-time PCR (qPCR) was performed using a CFX96 thermal cycler (Bio-Rad). Expression levels of target genes, including including Vascular Endothelial Growth Factor (VEGF), Fms-Like Tyrosine kinase 1 (FLT1), Fetal Liver Kinase 1 (FLK1), HemeOxygenase-1 (HO-1), interleukin-6 (IL-6), interleukin-8 (IL-8), endothelial Nitric Oxide Synthase (eNOS), inducible Nitric Oxide Synthase (iNOS), and Vascular Cell Adhesion Molecule-1 (VCAM-1), were analyzed using SYBR Green chemistry (8, 9, 11, 23–25), while reference genes (Glyceraldehyde-3-phosphate dehydrogenase, GAPDH; *β*-Actin, β-ACT) were assessed using TaqMan probes in multiplex reactions (26). Primer sequences, expected PCR product lengths, and NCBI accession numbers are shown in Table 2. Relative gene expression levels were normalized to the geometric mean of the two reference genes. The relative mRNA expression of the tested genes was calculated using the $2^{-\Delta\Delta CT}$ method (27) and referred to pAEC cultured under the standard condition (control).

TABLE 2 Primer sequence used for quantitative real time PCR analysis.

Gene	Sequence (5′-3′)	PCR (bp)	AN
VEGF	For: CCTTGCCTTGCTGCTCTACC Rev.: CGTCCATGAACTTCACCACTTC	101	AF318502
FLT1	For: TTGGACTGTTGGCACAAAGAC Rev.: GCTGTTGCTCGTCAGAATGG	141	AY566244
FLK1	For: AACGAGTGGAGGTGACAGATTG Rev.: CGGGTAGAAGCACTTGTAGGC	104	AJ245446
HO1	For: CGCTCCCGAATGAACAC Rev.: GCTCCTGCACCTCCTC	112	NM_00100402
IL-8	For: AGGACCAGAGCCAGGAAGAGAC Rev.: TGGAAAGGTGTGGAATGCGTATTTATG	203	AB057440.1
IL-6	For: AGCAAGGAGGTACTGGCAGAAAACAA Rev.: GTGGTGATTCTCATCAAGCAGGTCTCC	110	AF518322.1
VCAM-1	For: GAGGATGGAAGATTCTGGAATTTACG Rev.: ATCACTAGAGCAGGTCATGTTCAC	172	NM213891
iNOS	For: CAACAATGGCAACATCAGG Rev.: CATCAGGCATCTGGTAGC	119	U59390
eNOS	For: GCTCTCACCTTCTTCCTG Rev.: CCACTTCCACTCCTCATAG	144	AY266137
β-ACT	For: CTCGATCATGAAGTGCGACGT Rev.: GTGATCTCCTTCTGCATCCTGTC Probe: FAM-ATCAGGAAGGACCTCTACGCCAACACGG-BHQ1	114	KU672525.1
GAPDH	For: ACATGGCCTCCAAGGAGTAAGA Rev.: GATCGAGTTGGGGCTGTGACT Probe: HEX-CCACCAACCCCAGCAAGAGCACGC-BHQ1	106	NM_001206359

AN, accession number (NCBI).

2.13 Enzyme-linked immunosorbent assay (ELISA)

Porcine IL-8 concentrations in culture media were quantified using a commercial sandwich enzyme-linked immunosorbent assay (ELISA) kit (Elabscience). Cell culture supernatants were collected and immediately frozen at −80 °C after treatment with LPS (25 μg/mL) alone or in combination with VFM (1 mg/mL). 100 μL for each sample were used for the analysis. The assay sensitivity was 0.83 pg./mL, with a detection range of 1.56–100 pg./mL. Intra- and inter-assay coefficients of variation were <10%. Absorbance (450 nm) was measured using a microplate reader, and IL-8 concentrations were calculated from the standard curve generated for each assay.

2.14 *In vitro* capillary-like tube formation assay

The ability of pAEC to form capillary-like structures was evaluated using a tube formation assay on a three-dimensional extracellular matrix. Experiments were conducted in 8-well chamber slides coated with GelTrex™ Reduced Growth Factor Basement Membrane Matrix (Gibco, Thermo Fisher Scientific), as previously described (23). GelTrex™ was added to each well and allowed to polymerize for 30 min at 38.5 °C in a humidified atmosphere containing 5% CO_2. After polymerization, pAECs were seeded onto the matrix at a density of 1×10^5 cells/well. Cells were cultured in hESFM without FBS or antibiotics, to avoid interference with angiogenic responses. Cells were treated with VFM (0.1 or 1 mg/mL) and incubated under standard culture conditions. Images were acquired using a digital camera installed on a Nikon contrast phase microscope (Nikon, Yokohama, Japan). Quantitative analysis of tubular structures was performed using ImageJ 64 software with the Angiogenesis Analyzer plugin.

2.15 Animals

Male Balb/c mice (27.5 ± 2.5 g) were obtained from the Bioterium of Science Department of the Escuela Superior Politécnica de Chimborazo. They were group-housed in cages at temperature (24 ± 1 °C), constant humidity (55% ± 5%), and light–dark cycle (on at 7:00 a.m. and off at 7:00 p.m.). All animals were allowed *ad libitum* food and water according to the experimental protocols. Studies were performed in accordance with the NIH Guide for the Care and Use of Laboratory Animals, and the protocol was approved by the Ethics Committee of the Escuela Superior Politécnica de Chimborazo (ESPOCH-CIBE-2022-0037).

2.16 Carrageenan-induced mouse paw edema

Thirty mice were randomly divided into into six groups (5 mice/group): blank control, negative control (Carrageenan 1%), positive control (Carrageenan 1% + diclofenac suspension at 10 mg/kg), and experimental groups (Carrageenan 1% + VFM at 75, 150 and 300 mg/kg). Diclofenac and VFM were suspended in 0.5% w/v carboxymethylcellulose and administered orally 1 hour before carrageenan injection. Acute inflammation was produced by sub-plantar injection (25 μL) of 1% freshly prepared suspension of carrageenan into the right hind paw. Paw edema was assessed by measuring the thickness of the right hind paw using micrometer (Mitutoyo, Japan). Measurements were recorded in millimeters (mm) before carrageenan injection and at 1, 2, 3, 4, 5, and 6 h after carrageenan administration. The percentage inhibition of edema was calculated by comparison of the control group and experimental treatments as previously described (28, 29). At the end of the experiment, animals were euthanized using an intraperitoneal overdose of anesthetic (ketamine/xylazine, Agrovet-Market). This procedure was performed in accordance with international recommendations for the use and care of laboratory animals and to minimize pain, stress, and suffering.

2.17 Statistical analysis

Data were analysed by a one-way analysis of variance (one way ANOVA) followed by the "post-hoc" Tukey comparison Test or by Student's *t*-test, as appropriate. Differences of at least $p \leq 0.05$ were considered significant. Statistical analysis was carried out using GraphPad Prism 7 software.

3 Results

3.1 Structural and phytochemical characterization of VFM

The FTIR spectra of the extract before and after spray drying is presented in Figure 1. The most evident change was the attenuation of the broad O–H stretching band (3200–3,600 cm^{-1}) and the reduction in C=O stretching intensity (1700–1750 cm^{-1}) in the encapsulated sample. These shifts indicate hydrogen bonding interactions between polyphenols hydroxyl/carbonyl groups and maltodextrins, or steric shielding of reactive groups within the carbohydrate network (Figure 1). Through the microencapsulation process, a total of 19.07 g were recovered from 25.10 g of total solids initially fed into the spray dryer, resulting in a process yield of 75.97%.

A total of 17 compounds were identified and quantified in VFM, using HPLC–DAD and HPLC–MS analyses (Table 3). A diverse profile of secondary metabolites, specifically within the classes of procyanidins, flavonols, and dihydrochalcones, was found (Table 3). Procyanidin C1 (3.65 ppm) and procyanidin B2 (0.23 ppm) were considerably less abundant than procyanidin B1 (5.94 ppm). Quercetin (5.29 ppm) was the most common aglycone in the flavonol category while its glycoside counterpart hyperoside reached 2.68 ppm. In contrast, the glycosylated form kaempferol-7-*O*-glucoside (3.30 ppm) surpassed the aglycone kaempferol (1.82 ppm) for kaempferol derivatives. Interestingly, similar quantities of the dihydrochalcone phloretin and its 2′-glucoside phloridzin were detected (1.25 ppm). Lastly, the flavan-3-ol monomer epicatechin was detected at 1.13 ppm. Regarding the quantification of phenolic acids, chlorogenic acid was the most prevalent metabolite in VFM, with a concentration of 13.21 ppm. Protocatechuic acid, a hydroxybenzoic acid, followed next at 0.37 ppm. The concentrations of hydroxycinnamic acids, i.e., caffeic, ferulic, and *p*-coumaric acids were considerably lower and nearly equal at 0.27 ppm. The LC-MS analysis revealed the presence of cyanidine-3-*O*-galactoside and petunidin-3-*O*-glucoside as main anthocyanins in VFM, while cyanidin, delphinidin, and peonidin-3-*O*-glucoside were not detectable, being below the limit of quantification (Table 3).

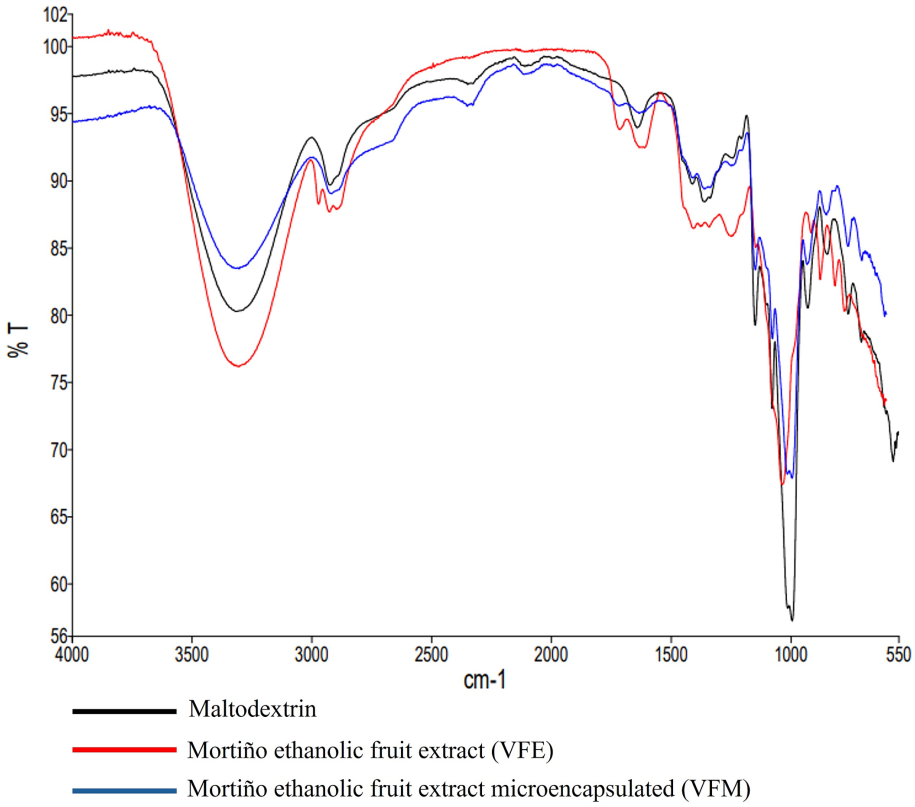

FIGURE 1
FTIR spectra before and after microencapsulation of mortiño fruit extract.

3.2 *In vitro* model

3.2.1 Angiogenesis

3.2.1.1 Effects of VFM on endothelial cell viability

Treatment of pAEC with VFM for 24 h did not negatively affect cell viability at any tested concentration. Nevertheless, exposure to VFM at 1 mg/mL (the highest concentration) significantly increased cell viability compared with the control condition ($p < 0.05$) (Figure 2).

3.2.1.2 Effects of VFM on angiogenesis-related gene expression

The expression of angiogenesis-related genes, including VEGF, its receptors FLK-1 (VEGFR-2) and FLT-1 (VEGFR-1), and HO-1, was evaluated at 5 h and 24 h following treatment with the phytoextract.

At 5 h (Figure 3A), a statistically significant effect was observed exclusively for FLT-1 expression showing an up-regulation of its gene expression in the presence of VFM at 0.1 mg/mL, whereas no significant difference was observed for other genes.

After 24 h of treatment, no differences were observed for the mRNA levels of studied genes (Figure 3B).

3.2.1.3 *In vitro* capillary-like tube formation assay

To investigate the pro-angiogenic potential of VFM, an *in vitro* capillary-like tube formation assay was performed on pAEC. Representative images obtained after 5 h of treatment with 1 mg/mL VFM showed well-defined capillary-like networks composed of interconnected junctions, segments, and meshes (Figure 4). All morphometric parameters were evaluated for untreated control cells (CTR) and for pAEC treated with VFM at concentrations of 0.1 mg/mL and 1 mg/mL, quantitative analysis revealed statistically significant differences between control and treated samples for all evaluated parameters (Figure 5).

3.2.2 *In vitro* inflammatory model

3.2.2.1 Effects of VFM on LPS-induced cell viability

The exposure to LPS (25 μg/mL) significantly reduced pAEC viability after 24 h ($p < 0.01$). The addition of VFM at high concentrations (1 mg/mL) to the culture system reduced LPS-induced cytotoxicity by restoring cell viability to basal levels; on the other hand, low concentrations of VFM (0.1 mg/mL) did not show to have any cytoprotective effect as cell viability was similar to cells only exposed to LPS and was significantly reduced compared to control cultures ($p < 0.05$) (Figure 6).

3.2.2.2 Effects of VFM on LPS-induced inflammatory marker expression

IL-6, IL-8, iNOS, and VCAM-1 mRNA levels were significantly upregulated when pAEC were exposed to LPS alone compared to control conditions after 5 h. The co-exposure of porcine endothelial cells to VFM (1 mg/mL) showed to partially counteract this LPS-induced

TABLE 3 Quantified phenolics and antioxidant activity in VFM through HPLC-DAD and HPLC/MS.

Class of compounds/ assay	Compound/ Assay	Concentration or activity
Phenolic acids	Protocatechuic acid	0.37 ± 0.17
	Caffeic acid	0.27 ± 0.07
	Chlorogenic acid	13.21 ± 2.01
	Ferulic acid	0.27 ± 0.01
	p-Coumaric acid	0.27 ± 0.02
Flavonoids	Quercetin	5.29 ± 0.10
	Quercetin-3-*O*-galactoside	2.68 ± 0.36
	Kaempferol	1.82 ±0.07
	Kaempferol-7-*O*-glucoside	3.30 ± 0.10
	Phloretin	1.25 ± 0.25
	Phloridzin	1.28 ± 0.25
	Epicatechin	1.13 ±0.17
	Procyanidin B1	5.94 ± 2.70
	Procyanidin B2	0.23 ± 0.01
	Procyanidin C1	3.65 ± 0.67
Anthocyanins	Cyanidin	N.D.
	Cyanidin-3-*O*-galactoside	2.58 ± 0.06
	Petunidin-3-*O*-glucoside	0.80 ± 0.01
	Peonidin-3-*O*-glucoside	N.D.
	Delphinidin	N.D.
Antioxidant activity	DPPH	38.86 ± 0.41
	ORAC	48.89 ± 1.73

The concentration of identified compounds is expressed as ppm ±SD; the antioxidant capacity is expressed as nmol Trolox equivalents/mg dry weight.

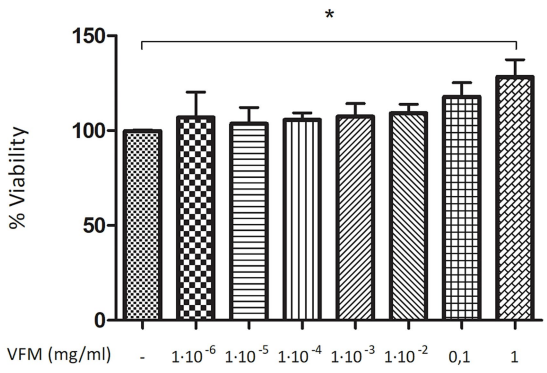

FIGURE 2
Effects of VFM on cell viability assessed by the MTT assay. PAECs were treated with increasing concentrations of VFM for 24 h. Statistical analysis was performed using Student's *t*-test comparing each treated group versus the untreated control (CTR). Data are presented as mean ± SEM. $n = 3$. CTR (–), untreated control; VFM, cells treated with the *Vaccinium floribundum* Kunth microencapsulated extract. *$p < 0.05$.

response: after 5 h the addition of VFM with LPS led to a significant reduction of pro-inflammatory markers (IL-6, IL-8, iNOS, and VCAM-1) compared to cells exposed to LPS alone (Figures 7A–C). The addition of VFM alone was able to significantly downregulate IL-8 gene expression levels compared to control cells (Figure 7A). eNOS gene expression was not altered in any culture conditions (Figure 7B).

3.2.2.3 IL-8 protein concentration in culture media

LPS stimulation significantly increased IL-8 protein concentration in cell culture medium compared with untreated control cell medium (CTR) ($p < 0.05$). Co-treatment with VFM (1 mg/mL) significantly reduced LPS-induced IL-8 protein concentration, restoring cytokine levels close to those observed in the control group ($p < 0.05$) (Figure 8).

3.3 *In vivo* model

3.3.1 Inflammatory inhibition

To compare the different treatments, the percentage of inflammation inhibition was calculated. The results showed that the positive control (Diclofenac) had an average inhibition of 51.74% ± 3.26%, while the microencapsulated group at 300 mg/kg had an average inhibition of 50.63% ± 1.66%. There were no significant differences ($p > 0.05$) between the diclofenac group and the VFM 300 mg/kg group, indicating that the anti-inflammatory effect of microencapsulation at this dose is comparable to that of the positive control treatment (Figure 9).

4 Discussion

For centuries, the local communities of Ecuador have leveraged the country's vast floral biodiversity for traditional medicinal applications. Within this ethnobotanical landscape, berries of *Vaccinium* spp. have gained global recognition as "superfruits," due to their antioxidant capacity and potential health benefits (30). The synergy between historical traditional use, cultural heritage, and the identification of potent bioactive constituents, such as polyphenols and anthocyanins, has catalyzed significant interest in the pharmacological and nutritional exploration of these species (31). For this reason, this study was designed to characterize the phytochemical profile and biological activity of a microencapsulated extract of *Vaccinium floribundum* Kunth (VFM), a species central to Ecuadorian traditional medicine. Specifically, we investigated the biological effects of VFM on primary porcine aortic endothelial cells (pAEC), focusing on its cytocompatibility, its role in promoting angiogenesis through the modulation of key molecular receptors, and its protective role against lipopolysaccharide (LPS)-induced endothelial dysfunction and inflammation. Furthermore, its anti-inflammatory potential was tested using an *in vivo* paw edema model which is a standardized acute, non-infectious model for inflammation. Microencapsulation represents an advanced delivery strategy designed to enhance the physicochemical stability of bioactive compounds by forming a protective matrix that limits environmental exposure (32). This approach is particularly relevant for phenolic compounds, which hydroxyl groups and conjugated

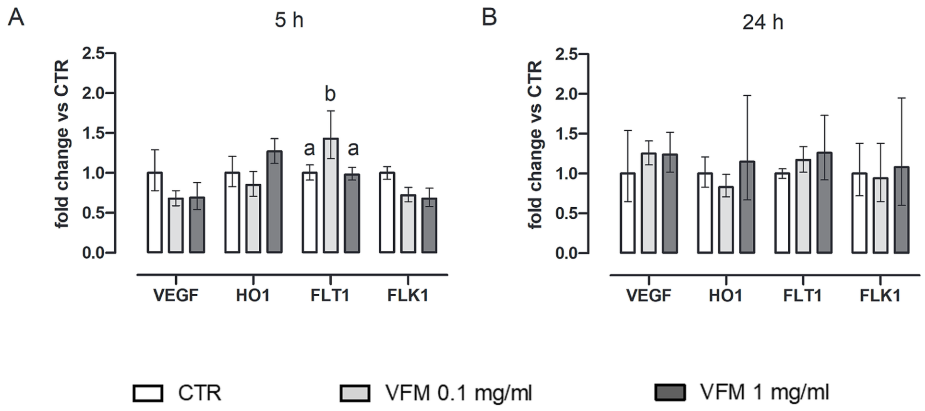

FIGURE 3
Effect of VFM treatment on angiogenesis-related gene expression. Expression of VEGF, HO-1, FLT-1 (VEGFR-1), and FLK-1 (VEGFR-2) was evaluated by qPCR after 5 h **(A)** and 24 h **(B)** of treatment with VFM (0.1 mg/mL and 1 mg/mL). Gene expression levels are reported as fold change ($2^{-\Delta\Delta Ct}$) in respect to the control cells. Error bar represents the range of relative gene expression (n = 3). Statistical analysis was performed using one-way ANOVA, followed by appropriate post-hoc multiple comparison tests. Different letters indicate statistically significant differences among groups ($p < 0.05$). CTR, untreated control; VFM, *Vaccinium floribundum Kunth* microencapsulated extract.

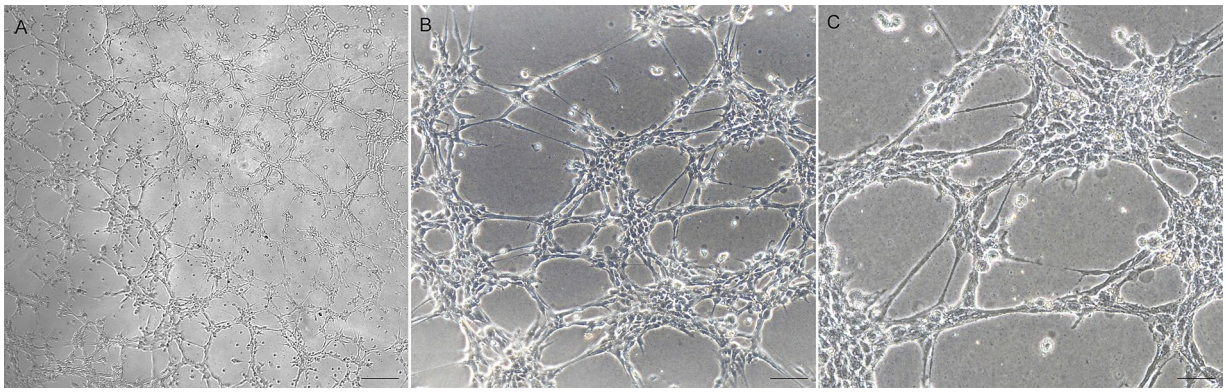

FIGURE 4
Representative phase-contrast images of tubular structure formation in pAECs treated with VFM at 1 mg/mL (VFM 1) after 5 h of incubation: **(A)** Scale bar = 500 µm; **(B)** Scale bar = 100 µm; **(C)** Scale bar = 50 µm.

structures are highly susceptible to photodegradation, thermal instability, and oxidative stress. Thus, the protective barrier former mitigates the formation of reactive oxygen species and preserves the intrinsic antioxidant and anti-inflammatory properties of the encapsulated compounds (18).

The spray drying process yielded results consistent with those reported for polysaccharide-based delivery systems. However, yield should not be correlated with encapsulation efficiency or loading capacity, since these require targeted analytical assessment of bioactive retention within the particles (33). FTIR analysis revealed spectral features characteristic of polyphenol–polysaccharide interactions, including enhanced absorption bands within the 1,050–1,160 cm^{-1} region attributed to C–O–C glycosidic linkages and C–O stretching vibrations. The increased intensity and structural reinforcement of these bands further supported the stabilizing contribution of maltodextrin as a carrier matrix (34).

The phenolics profile observed in VFM was characterized by the dominance of B-type procyanidins, quercetin-based flavonols, and chlorogenic acid. The high concentration of Procyanidin B1 relative to B2 and C1 suggested a biosynthetic preference for specific dimeric structures, which are critical for the fruit's astringency and the antioxidant capacity (35). The lower levels of procyanidin C1 (a trimer) compared to the B1 dimer reflected the typical oligomerization gradient where dimers are more prevalent than higher-order trimers (36). The flavonol profile was dominated by quercetin and its galactoside derivative. Blueberries are well-documented sources of quercetin, a potent anti-inflammatory agent, typically containing about 100 mg/kg (37). The presence of hyperoside (quercetin-3-*O*-galactoside) aligned with the plant's tendency to store flavonols in glycosylated forms to increase stability and solubility (38). Likewise, the higher levels of kaempferol-7-*O*-glucoside compared to its aglycone reflected this metabolic storage strategy. The detection of phloretin and phloridzin was significant as these dihydrochalcones were more famously associated with apples, yet they were increasingly identified in blueberries as minor but potent bioactive markers (39). Furthermore, the levels of epicatechin provided the necessary substrate for the condensed tannins (procyanidins) identified, indicating a highly active flavonoid pathway (40). The dominance of chlorogenic acid aligned with its role as the hallmark antioxidant in blueberries, often constituting the majority of the total phenolic acid fraction (41). Its high concentration relative to its precursor, caffeic acid, indicated a high rate of esterification with quinic acid within the fruit's

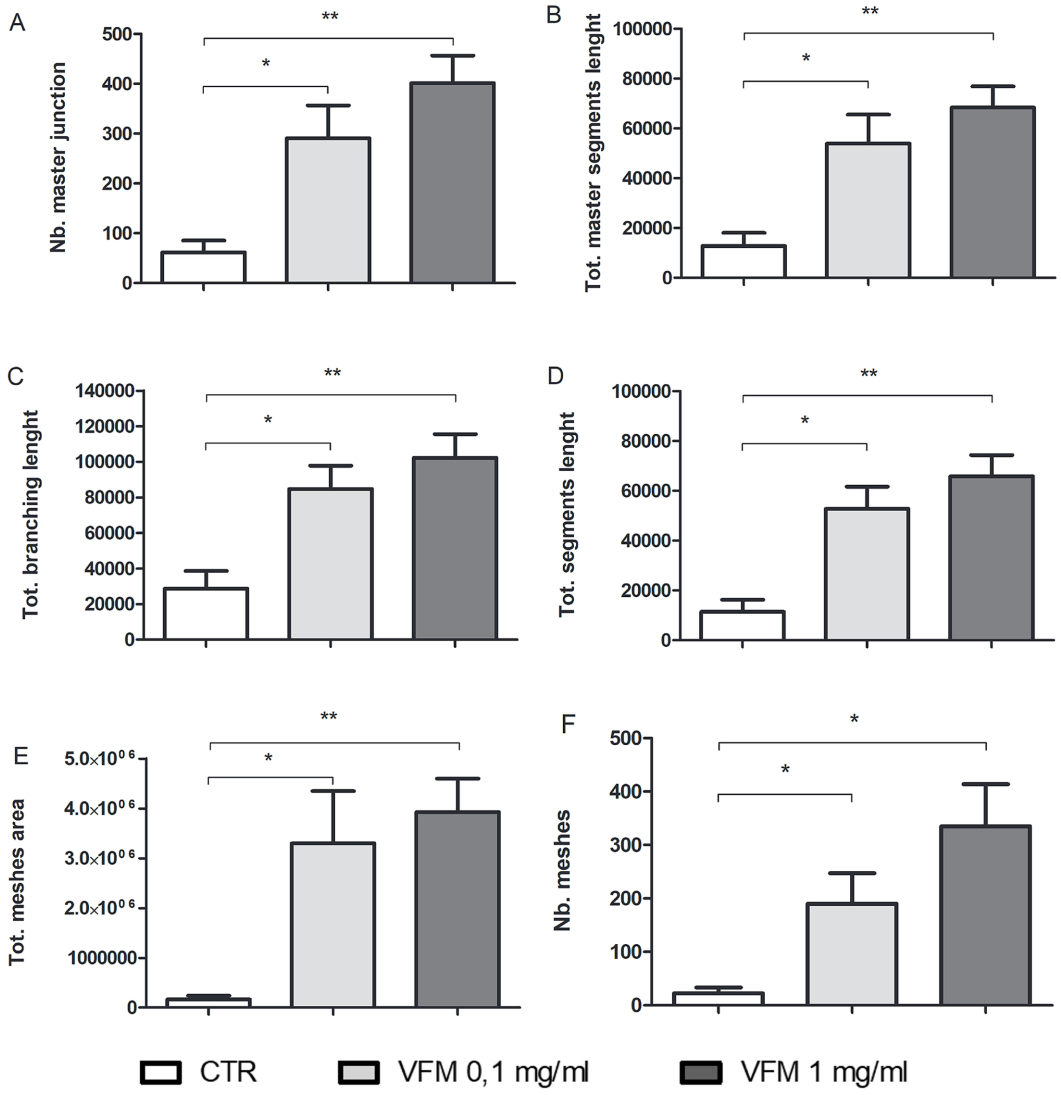

FIGURE 5
In vitro capillary-like tube formation assay following VFM treatment. Morphometric analysis of capillary-like networks formed by pAECs treated with VFM (0.1 mg/mL and 1 mg/mL), compared with control (CTR). Quantitative parameters include: **(A)** Number of master junctions; **(B)** total master segment length; **(C)** total branching length; **(D)** total segment length; **(E)** total mesh area; and **(F)** number of meshes. Data are expressed as mean ± SEM ($n = 3$). Image analysis was performed using the Angiogenesis Analyzer plugin (ImageJ). Statistical analysis was performed using Student's *t*-test. Asterisks indicate significance versus control: $*p < 0.05$ and $**p < 0.005$.

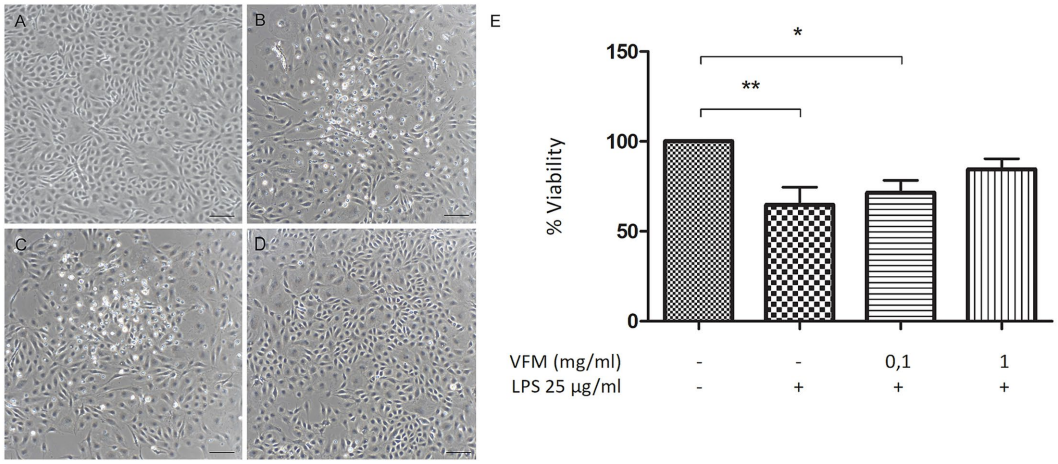

FIGURE 6
Effects of lipopolysaccharide (LPS) and *Vaccinium floribundum* Kunth microencapsulated extract (VFM) on cell morphology (**A**: Control pAEC; **B**: LPS stimulation; **C**, **D**: co-treatment with LPS and VFM 0,1 and 1 mg/ml respectively.) and on cell viability as assessed by the MTT assay (**E**). Statistical analysis was performed using one-way ANOVA. $*p < 0.05$; $**p < 0.01$. Data are presented as mean ± SEM. $n = 5$.

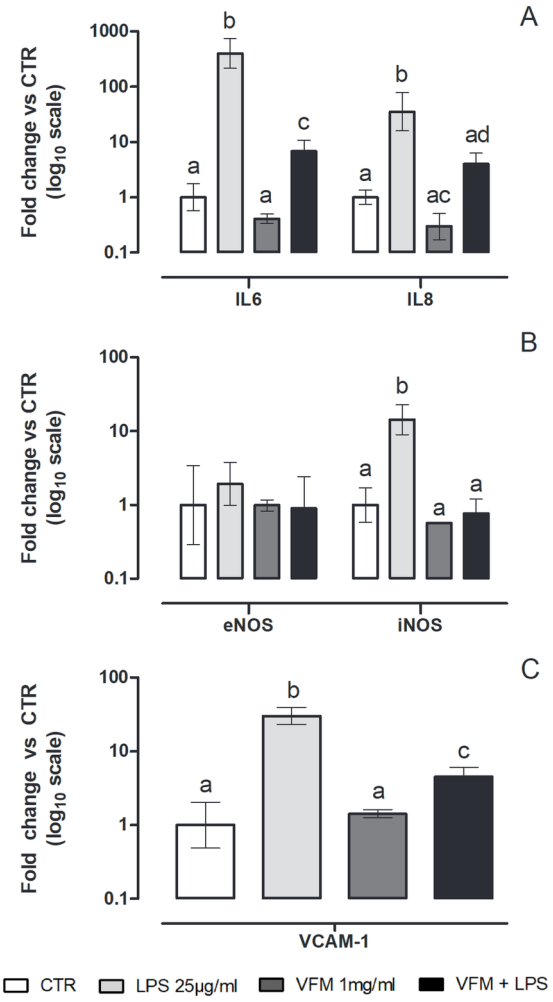

FIGURE 7
Effect of VFM on LPS-induced IL-6 and IL-8 **(A)**, eNOS and iNOS **(B)**, and VCAM-1 **(C)** gene expression. Relative mRNA levels of IL-6, IL-8, eNOS, iNOS, and VCAM-1 were quantified by RT–qPCR at 5 h. Cells were treated with lipopolysaccharide (LPS 25 µg/mL) alone or in combination with VFM at the indicated concentration (1 mg/mL). Gene expression levels are reported as fold change relative to the control ($2^{-\Delta\Delta Ct}$ method) and presented on a log10 scale. Error bars represent the range of relative gene expression ($n = 3$). Values not sharing a common letter indicate statistically significant differences ($p < 0.05$) among experimental groups, as determined by one-way ANOVA followed by Tukey's post-hoc multiple comparisons test. CTR, untreated control; LPS, lipopolysaccharide; VFM, Vaccinium floribundum Kunth microencapsulated extract.

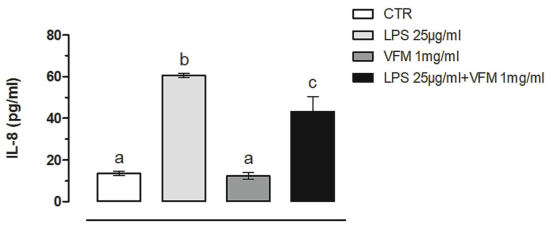

FIGURE 8
Effects of LPS and VFM on IL-8 protein concentration. IL-8 protein concentration in culture media were determined by ELISA after treatment with LPS (25 µg/mL) alone or in combination with VFM (1 mg/mL). Data represent the mean ± SD of 3 replicates. Different letters indicate statistically significant differences among experimental groups ($p < 0.05$), as determined by one-way ANOVA followed by Tukey's post-hoc multiple comparisons test. CTR, untreated control; LPS, lipopolysaccharide; VFM, *Vaccinium floribundum* Kunth microencapsulated extract; pAEC, porcine aortic endothelial cells.

metabolic pathways (19). The uniform, low levels of ferulic and *p*-coumaric acids suggested that these compounds served primarily as transient intermediates in the biosynthesis of more complex polyphenols or were integrated into the cell wall matrix (42). Meanwhile, the detection of protocatechuic acid was noteworthy as it often emerged from the degradation of anthocyanins or existed as a biosynthetic precursor to gallic acid derivatives (43).

The preliminary safety screening confirmed that VFM is highly cytocompatible with porcine aortic endothelial cells (pAEC). In fact, treatment of pAEC with VFM for 24 h did not negatively affect cell viability at any of the concentrations tested. Most importantly, at 1 mg/mL, VFM significantly enhanced cell metabolic activity. Therefore, the increased cell viability might suggest that VFM could actively support endothelial health and metabolic vigor. The observed bioactivity of VFM is likely due to the high content of polyphenols and anthocyanins found in *Vaccinium* species, which have been shown to modulate metabolic pathways and reduce oxidative stress in vascular models (44, 45).

Following the preliminary assay, pAEC angiogenesis potential was evaluated using an *in vitro* extracellular matrix-based assay widely recognized for evaluating the ability of endothelial cells to organize into complex structures. The formation of new vascular networks is a multi-step process that requires the transition of endothelial cells from a quiescent state to an active, migratory, and organizational phenotype.

Our results demonstrate that VFM treatment significantly promotes the organizational capacity of pAEC. This is evidenced by a substantial increase in all evaluated morphometric parameters, including master junctions, total segment length, and mesh area (Figure 5). The fact that the extract enhances the complexity of the capillary-like network across all metrics suggests that VFM does not merely stimulate random migration but actively orchestrates the cellular interactions necessary for structural stabilization. Interestingly, this morphological transformation was accompanied by a specific and transient transcriptional response. At the 5-h mark, a significant up-regulation was observed exclusively for the FLT-1 (VEGFR-1) receptor. By 24 h, the mRNA levels of all tested markers, including VEGF, FLK-1 (VEGFR-2), and HO-1, returned to baseline. In vascular biology, FLT-1 and FLK-1 are considered "early molecular switches" that trigger the endothelial-to-angiogenic transition. Given that FLT-1 plays a crucial role in guidance and spatial organization during the initial phases of vessel assembly. However, the return to baseline levels for all genes by 24 h suggests that the 5-h time point may represent the tail end of this initial transcriptional wave. Consequently, the observed lack of significant modulation at 24 h, and the partial response at 5 h indicates that VFM initiates a rapid signaling cascade. Future studies should focus on earlier time points, such as 3 h, to capture the peak expression of this "angiogenic switch" and fully characterize the kinetics of VFM-mediated endothelial activation.

Overall, our results concerning angiogenesis are in agreement with the proangiogenic potential of polyphenols and their ability to orchestrate complex molecular signalling pathways that promoted the growth and stabilization of vascular networks (46). These natural compounds have been reported to regulate various stages of angiogenesis, including the modulation of factors such as basic fibroblast growth factor [bFGF: (47)], vascular endothelial growth factor [VEGF: (48, 49)], hypoxia-inducible factor-1α [HIF-1α: (50)], and matrix metalloproteinase

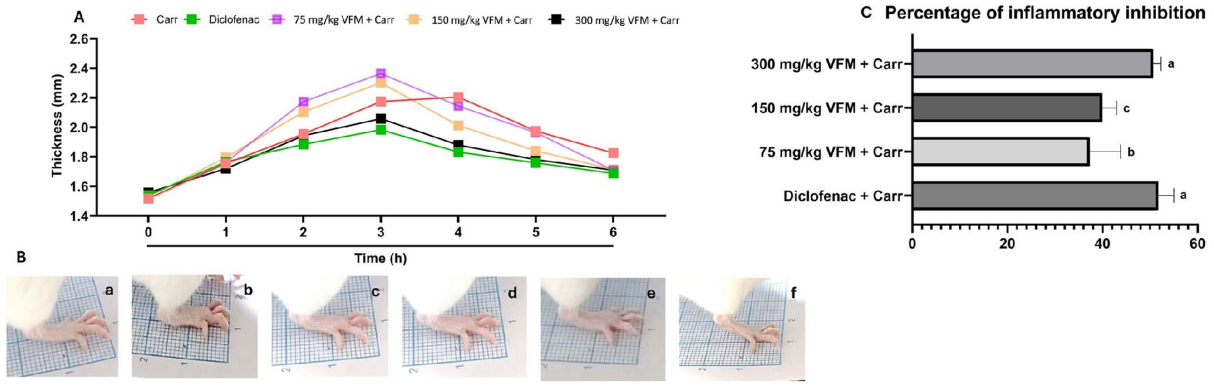

FIGURE 9
Effect of *Vaccinium floribundum* Kunth microencapsulated extract (VFM) in mice (n = 5) by carrageenan paw edema assay. The thickness of paw (mm) was measured at 1, 2, 3, 4, 5 and 6 h after the injection of Carr, respectively, **(A)**. Effects of VFM on the inflammatory response at 6 h **(B)**, control group (a), Carr group (b), Diclofenac group + Carr (c), 75 mg/kg VFM + Carr (d), 150 mg/kg VFM + Carr (e), 300 mg/kg VFM + Carr (f). Percentage of inflammatory inhibition **(C)**. Statistical analysis was performed using one-way ANOVA and Dunnet *post hoc*-test. Data are presented as mean ± SD. n = 5.

(MMP) activity (51). Moreover, they also influence endothelial cell functions, including proliferation, migration, and tube formation (52) and references therein, thereby impacting tumor vascularization and metastatic potential (53), as well as vascular-associated complications. Several studies carried out both *in vivo* and *in vitro* have demonstrated that angiogenesis represent a therapeutic target for plant polyphenols (52). These compounds, specifically at low doses, activated critical receptors such as VEGFR, EGFR, and the ANG 1/2/tyrosine kinase system, essential for endothelial cell proliferation and migration (54). Among polyphenol compounds detected in VFM, delphinidin is primarily recognized for its anti-angiogenic properties in cancer contexts, it could exhibit a pro-angiogenic or vasculoprotective effect under specific physiological conditions, often characterized by a biphasic (dose-dependent) response. At low concentrations, delphinidin and similar anthocyanidins could promote the release of nitric oxide (NO) from endothelial cells (55), enhanced blood flow and might support healthy vessel maintenance or repair in ischemic tissues through the activation of oestrogen receptor alpha (ERα) (56). Essentially, it acted as a modulator that suppressed abnormal vessel growth while potentially supporting the integrity of existing healthy vasculature by supporting basal mitochondrial DNA and mRNA expression of factors like NRF1 and Tfam in normal cells (57).

Lipopolysaccharide (LPS) is a well-established inducer of endothelial dysfunction, triggering an inflammatory response along with oxidative stress, resulting in high cell death rate due to the cytotoxic environment (58). In the present study, LPS exposure significantly reduced endothelial cells viability, which might confirm the presence of an inflammatory microenvironment. Notably, high doses of VFM (1 mg/mL) restored cell viability almost to basal levels after 24 h. This cytoprotective effect could be ascertained to the high concentrations of flavonoids and anthocyanins contained in VFM, which have been identified in the herein described extract (59–61). Indeed, the cytoprotection provided by mortiño extracts might be also reflected by the gene expression of pro-inflammatory interleukins mRNA levels (IL-6 and IL-8) or protein levels (IL-8) as high doses of VFM significantly down-regulated their expression compared to pAEC exposed only to LPS for 5 h. Furthermore, VFM was able to downregulate the gene expression of VCAM-1 and iNOS after exposure to LPS; both are two important markers with a critical role in endothelial biology, especially during inflammation (62, 63). Indeed, high doses of VFM showed to diminish the mRNA levels of iNOS and VCAM-1 in the presence of LPS compared to treatment with LPS alone, with the former presenting basal levels comparable to physiological conditions of culture. The higher levels of iNOS might have been one of the effectors inducing the expression of interleukins due to the higher levels of nitric oxide (NO) (64), in addition to the direct effects of LPS on endothelial cells physiology. The addition of VFM reduced the gene expression of all these factors, along with the presence of IL-8 in the cell culture medium. Similarly, a diminished expression of VCAM-1 after exposure to VFM could be related to the protective effects of berry extracts towards LPS along with the lower presence of iNOS and pro-inflammatory cytokines (58). Different studies have demonstrated that blueberries extract, due to the presence of compounds such as polyphenols, are able to modulate inflammatory and oxidative environments in complex biological systems (45, 65–67). As a matter of fact, the bioactive constituents present in the mortiño fruit extract, namely flavonoids and anthocyanins, are known for being able to modulate the protective endogenous oxidative stress machinery of cells by upregulating the gene expression of nuclear factor erythroid 2-like 2 (Nfr2) (68) or by inhibiting NF-κB signaling pathway in endothelial cells (69–71) or blocking the same pathway along with the AMPK signalling one, which is a known mechanism of action of quercetin flavonols (72–74). These mechanisms together might have led to the observed reduction of inflammation within LPS-stimulated pAEC, which showed a downregulated expression of IL-6, IL-8 (both at the mRNA and protein level), iNOS, and VCAM-1 after 5 h in culture, along with the increased pAECs viability after exposure to LPS compared to LPS alone.

Finally, the results concerning *in vivo* model of acute inflammation by using the carrageenan-induced paw edema assay (75–77) demonstrated the anti-inflammatory property of VFM. In particular, following carrageenan administration, a rapid inflammatory response occurred, characterized by edema, hyperalgesia, and erythema due to the release of several pro-inflammatory mediators including histamine, complement components, and pro-inflammatory cytokines (78). In the present study, all tested concentrations of the extract exhibited anti-inflammatory activity, with the highest dose (300 mg/kg) producing the most pronounced reduction in paw edema. These findings are consistent with previous reports describing anti-inflammatory properties in other species of the *Vaccinium* genus. For instance, Nardi et al. (79) reported that extracts of *Vaccinium myrtillus* and *Vaccinium macrocarpon*, administered orally at 200 mg/kg, reduced carrageenan-induced paw edema by

28.8% and 36.9%, respectively (79). Even though the anti-inflammatory effect observed for VFM is consistent with the bioactivity of polyphenol-rich *Vaccinium* species extracts, this study cannot establish a direct causal relationship between microencapsulation and the *in vivo* response. Therefore, future formulation-focused studies should compare VFM with the corresponding free extract and assess encapsulation efficiency, loading capacity, phenolic/anthocyanin retention, stability, and release behavior. Furthermore, a larger cohort of animals and target-species studies will be fundamental in the future for assessing the direct therapeutic efficacy of the mortiño extract in a clinical setting. Nonetheless, this study is a first step in the development pipeline of a potential therapeutic evaluation.

In conclusion, the microencapsulated *Vaccinium floribundum* Kunth extract (VFM) demonstrated robust pro-angiogenic and anti-inflammatory activities in both *in vitro* and *in vivo* models. VFM effectively enhanced endothelial cell viability, promoted capillary-like network formation, and modulated early angiogenic signaling pathways, highlighting its promising role in supporting vascular health. Moreover, VFM mitigated LPS-induced endothelial dysfunction by downregulating pro-inflammatory cytokines, consistent with the known bioactivity of polyphenols and anthocyanins. The *in vivo* model supported VFM antiflammatory activity: Altogether, these findings provide a preliminary scientific basis for the traditional use of *Vaccinium floribundum* in Ecuadorian ethnomedicine, highlighting the relevance of the traditional knowledge and supporting the sustainable use of natural resources in a country characterized by high biodiversity. Future perspectives may include the development of a VFM-based nutraceutical formulation targeting vascular and inflammatory disorders along with mechanistic and more complex model studies, although this will require overcoming the limitations usually associated with wild plant harvesting, ensuring the production of standardized and more chemically stable extract.

Data availability statement

The datasets presented in this study can be found in online repositories. The names of the repository/repositories and accession number(s) can be found in the article/supplementary material. The datasets VFM-pAEC for this study can be found in the AMSACTA from the University of Bologna https://amsacta.unibo.it/id/eprint/8873.

Ethics statement

The animal study was approved by Ethics Committee of the Escuela Superior Politécnica de Chimborazo (ESPOCH-CIBE-2022-0037). The study was conducted in accordance with the local legislation and institutional requirements.

Author contributions

FA: Funding acquisition, Resources, Formal analysis, Writing – original draft, Validation, Supervision, Writing – review & editing, Conceptualization. IT: Supervision, Validation, Formal analysis, Resources, Conceptualization, Writing – review & editing, Writing – original draft, Funding acquisition. GB: Formal analysis, Writing – review & editing, Methodology, Writing – original draft, Investigation, Data curation. LM: Formal analysis, Data curation, Methodology, Writing – review & editing, Writing – original draft, Investigation. RDL: Data curation, Writing – review & editing, Methodology, Investigation. SA: Writing – review & editing, Validation, Investigation, Writing – original draft, Methodology, Data curation. RS: Writing – review & editing, Investigation, Data curation, Methodology. GV: Writing – review & editing, Investigation. CG: Data curation, Methodology, Writing – review & editing, Investigation. GC: Data curation, Investigation, Methodology, Writing – review & editing. MF: Writing – review & editing, Investigation. AZ: Formal analysis, Resources, Data curation, Supervision, Methodology, Writing – review & editing, Investigation, Funding acquisition. CB: Data curation, Conceptualization, Resources, Validation, Supervision, Methodology, Funding acquisition, Investigation, Writing – review & editing, Formal analysis.

Funding

The author(s) declared that financial support was received for this work and/or its publication. This study was supported by Escuela Superior Politécnica de Chimborazo (Ecuador) through the project IDIPI-333 and by Ricerca Fondamentale Orientata (RFO) 2025 grants from the University of Bologna (Italy) to AZ, CB, FA.

Conflict of interest

The author(s) declared that this work was conducted in the absence of any commercial or financial relationships that could be construed as a potential conflict of interest.

Generative AI statement

The author(s) declared that Generative AI was not used in the creation of this manuscript.

Any alternative text (alt text) provided alongside figures in this article has been generated by Frontiers with the support of artificial intelligence and reasonable efforts have been made to ensure accuracy, including review by the authors wherever possible. If you identify any issues, please contact us.

Publisher's note

References

1. Atanasov AG, Waltenberger B, Pferschy-Wenzig EM, Linder T, Wawrosch C, Uhrin P, et al. Discovery and resupply of pharmacologically active plant-derived natural products: a review. *Biotechnol Adv*. (2015) 33:1582–614. doi: 10.1016/j.biotechadv.2015.08.001

2. Jeong JH, Ojha U, Lee YM. Pathological angiogenesis and inflammation in tissues. *Arch Pharm Res*. (2021) 44:1–15. doi: 10.1007/s12272-020-01287-2

3. Totoń-Żurańska J, Mikolajczyk TP, Saju B, Guzik TJ. Vascular remodelling in cardiovascular diseases: hypertension, oxidation, and inflammation. *Clin Sci*. (2024) 138:817–50. doi: 10.1042/CS20220797

4. Medzhitov R. The spectrum of inflammatory responses. *Science*. (2021) 374:1070–5. doi: 10.1126/science.abi5200

5. Bernardette Martínez-Rizo A, Fosado-Rodríguez R, César Torres-Romero J, César Lara-Riegos J, Alberto Ramírez-Camacho M, Ly Arroyo Herrera A, et al. Models *in vivo* and *in vitro* for the study of acute and chronic inflammatory activity: a comprehensive review. *Int Immunopharmacol*. (2024) 135:112292. doi: 10.1016/j.intimp.2024.112292

6. Rafiyan M, Sadeghmousavi S, Akbarzadeh M, Rezaei N. Experimental animal models of chronic inflammation. *Curr Res Immunol*. (2023) 4:100063. doi: 10.1016/j.crimmu.2023.100063

7. Seok J, Warren HS, Cuenca AG, Mindrinos MN, Baker HV, Xu W, et al. Genomic responses in mouse models poorly mimic human inflammatory diseases. *Proc Natl Acad Sci USA*. (2013) 110:3507–12. doi: 10.1073/pnas.1222878110

8. Tubon I, Bernardini C, Antognoni F, Mandrioli R, Potente G, Bertocchi M, et al. *Clinopodium tomentosum* (Kunth) Govaerts leaf extract influences in vitro cell proliferation and angiogenesis on primary cultures of porcine aortic endothelial cells. *Oxidative Med Cell Longev*. (2020) 2020:1–11. doi: 10.1155/2020/2984613

9. Tubon I, Zannoni A, Bernardini C, Salaroli R, Bertocchi M, Mandrioli R, et al. In vitro anti-inflammatory effect of *Salvia sagittata* Ethanolic extract on primary cultures of porcine aortic endothelial cells. *Oxidative Med Cell Longev*. (2019) 2019:1–11. doi: 10.1155/2019/6829173

10. Bertocchi M, Isani G, Medici F, Andreani G, Tubon Usca I, Roncada P, et al. Anti-inflammatory activity of *Boswellia serrata* extracts: an in vitro study on porcine aortic endothelial cells. *Oxidative Med Cell Longev*. (2018) 2018:2504305. doi: 10.1155/2018/2504305

11. Bernardini C, Greco F, Zannoni A, Bacci ML, Seren E, Forni M. Differential expression of nitric oxide synthases in porcine aortic endothelial cells during LPS-induced apoptosis. *J Inflamm Lond Engl*. (2012) 9:47. doi: 10.1186/1476-9255-9-47

12. Vasco C, Riihinen K, Ruales J, Kamal-Eldin A. Chemical composition and phenolic compound profile of Mortiño (*Vaccinium floribundum* Kunth). *J Agric Food Chem*. (2009) 57:8274–81. doi: 10.1021/jf9013586

13. Llivisaca S, Manzano P, Ruales J, Flores J, Mendoza J, Peralta E, et al. Chemical, antimicrobial, and molecular characterization of mortiño (*Vaccinium floribundum* Kunth) fruits and leaves. *Food Sci Nutr*. (2018) 6:934–42. doi: 10.1002/fsn3.638

14. Schreckinger ME, Lotton J, Lila MA, de Mejia EG. Berries from South America: a comprehensive review on chemistry, health potential, and commercialization. *J Med Food*. (2010) 13:233–46. doi: 10.1089/jmf.2009.0233

15. Botanic Gardens of Sydney. Microsoft Word - How to collect plants.doc. Available online at: https://www.botanicgardens.org.au/sites/default/files/2023-06/How-to-collect-plants.pdf (Accessed March 18, 2026).

16. Das PE, Majdalawieh AF, Abu-Yousef IA, Narasimhan S, Poltronieri P. Use of a hydroalcoholic extract of *Moringa oleifera* leaves for the green synthesis of bismuth nanoparticles and evaluation of their anti-microbial and antioxidant activities. *Materials*. (2020) 13:876. doi: 10.3390/ma13040876

17. da Righi Rosa J, Nunes GL, Motta MH, Fortes JP, Cezimbra Weis GC, Rychecki Hecktheuer LH, et al. Microencapsulation of anthocyanin compounds extracted from blueberry (*Vaccinium* spp.) by spray drying: characterization, stability and simulated gastrointestinal conditions. *Food Hydrocoll*. (2019) 89:742–8. doi: 10.1016/j.foodhyd.2018.11.042

18. Barba-Ostria C, López O, Debut A, Mayorga-Ramos A, Zúñiga-Miranda J, Coyago-Cruz E, et al. Bioactive phenolic compounds from Rambutan (*Nephelium lappaceum* L.) shell: encapsulation, structural stability, and multifunctional activities. *Int J Mol Sci*. (2025) 26:10859. doi: 10.3390/ijms262210859

19. Mattila P, Hellström J, Törrönen R. Phenolic acids in berries, fruits, and beverages. *J Agric Food Chem*. (2006) 54:7193–9. doi: 10.1021/jf0615247

20. Antognoni F, Potente G, Biondi S, Mandrioli R, Marincich L, Ruiz KB. Free and conjugated phenolic profiles and antioxidant activity in quinoa seeds and their relationship with genotype and environment. *Plants*. (2021) 10:1046. doi: 10.3390/plants10061046

21. Wojdyło A, Nowicka P, Laskowski P, Oszmiański J. Evaluation of sour cherry (*Prunus cerasus* L.) fruits for their polyphenol content, antioxidant properties, and nutritional components. *J Agric Food Chem*. (2014) 62:12332–45. doi: 10.1021/jf504023z

22. Bernardini C, Mantia DL, Salaroli R, Ventrella D, Elmi A, Zannoni A, et al. Isolation of vascular wall mesenchymal stem cells from the thoracic aorta of adult Göttingen Minipigs: a new protocol for the simultaneous endothelial cell collection. *Anim Open Access J MDPI*. (2023) 13:2601. doi: 10.3390/ani13162601

23. Bernardini C, Zannoni A, Bertocchi M, Tubon I, Fernandez M, Forni M. Water/ethanol extract of *Cucumis sativus* L. fruit attenuates lipopolysaccharide-induced inflammatory response in endothelial cells. *BMC Complement Altern Med*. (2018) 18:194. doi: 10.1186/s12906-018-2254-1

24. Zaniboni A, Bernardini C, Bertocchi M, Zannoni A, Bianchi F, Avallone G, et al. In vitro differentiation of porcine aortic vascular precursor cells to endothelial and vascular smooth muscle cells. *Am J Physiol Cell Physiol*. (2015) 309:C320–31. doi: 10.1152/ajpcell.00049.2015. PMID: 26135800

25. Botelho G, Bernardini C, Zannoni A, Ventrella V, Bacci ML, Forni M. Effect of tributyltin on mammalian endothelial cell integrity. *Comp Biochem Physiol Part C Toxicol Pharmacol*. (2015) 176–177:79–86. doi: 10.1016/j.cbpc.2015.07.012

26. Duvigneau JC, Hartl RT, Groiss S, Gemeiner M. Quantitative simultaneous multiplex real-time PCR for the detection of porcine cytokines. *J Immunol Methods*. (2005) 306:16–27. doi: 10.1016/j.jim.2005.06.021

27. Livak KJ, Schmittgen TD. Analysis of relative gene expression data using real-time quantitative PCR and the $2^{-\Delta\Delta CT}$ method. *Methods*. (2001) 25:402–8. doi: 10.1006/meth.2001.1262

28. Patriota LLS, Ramos DBM, Silva MG, Santos ACLA, Silva YA, Paiva PMG, et al. Inhibition of carrageenan-induced acute inflammation in mice by the *Microgramma vacciniifolia* frond lectin (MvFL). *Polymers*. (2022) 14:1609. doi: 10.3390/polym14081609

29. Sharma JN, Samud AM, Asmawi MZ. Comparison between plethysmometer and micrometer methods to measure acute paw oedema for screening anti-inflammatory activity in mice. *Inflammopharmacology*. (2004) 12:89–94. doi: 10.1163/156856004773121400

30. Llivisaca-Contreras SA, León-Tamariz F, Manzano-Santana P, Ruales J, Naranjo-Morán J, Serrano-Mena L, et al. Mortiño (*Vaccinium floribundum* Kunth): an underutilized superplant from the Andes. *Horticulturae*. (2022) 8:358. doi: 10.3390/horticulturae8050358

31. Caranqui-Aldaz JM, Muelas-Domingo R, Hernández F, Martínez R. Chemical composition and polyphenol compounds of *Vaccinium floribundum* Kunth (Ericaceae) from the volcano Chimborazo Paramo (Ecuador). *Horticulturae*. (2022) 8:956. doi: 10.3390/horticulturae8100956

32. Szpicer A, Bińkowska W, Stelmasiak A, Wojtasik-Kalinowska I, Czajkowska A, Mierzejewska S, et al. Innovative microencapsulation techniques of bioactive compounds: impact on physicochemical and sensory properties of food products and industrial applications. *Appl Sci*. (2025) 15:11908. doi: 10.3390/app152211908

33. Emon DD, Islam MDS, Mazumder MAR, Aziz MG, Rahman MS. Recent applications of microencapsulation techniques for delivery of functional ingredient in food products: a comprehensive review. *Food Chem Adv*. (2025) 6:100923. doi: 10.1016/j.focha.2025.100923

34. Ingale OS, Pravin BP, Pawase PA, Shams R, Dash KK, Bashir O, et al. Enhancing bioactive stability and applications: microencapsulation in fruit and vegetable waste valorization. *Discov Food*. (2025) 5:148. doi: 10.1007/s44187-025-00412-8

35. Määttä-Riihinen KR, Kähkönen MP, Törrönen AR, Heinonen IM. Catechins and procyanidins in berries of *vaccinium* species and their antioxidant activity. *J Agric Food Chem*. (2005) 53:8485–91. doi: 10.1021/jf050408l

36. Phansalkar RS, Nam JW, Leme AA, Gan LS, Zhou B, McAlpine JB, et al. Proanthocyanidin dimers and trimers from *Vitis vinifera* provide diverse structural motifs for the evaluation of dentin biomodification. *J Nat Prod*. (2019) 82:2387–99. doi: 10.1021/acs.jnatprod.8b00953

37. Erlund I, Freese R, Marniemi J, Hakala P, Alfthan G. Bioavailability of quercetin from berries and the diet. *Nutr Cancer*. (2006) 54:13–7. doi: 10.1207/s15327914nc5401_3

38. Veitch NC, Grayer RJ. Flavonoids and their glycosides, including anthocyanins. *Nat Prod Rep*. (2008) 25:555–611. doi: 10.1039/B718040N

39. Kahle K, Kraus M, Scheppach W, Ackermann M, Ridder F, Richling E. Studies on apple and blueberry fruit constituents: Do the polyphenols reach the colon after ingestion? *Mol Nutr Food Res*. (2006) 50:418–23. doi: 10.1002/mnfr.200500211

40. Rauf A, Imran M, Abu-Izneid T, Iahtisham-Ul-Haq, Patel S, Pan X, et al. Proanthocyanidins: a comprehensive review. *Biomed Pharmacother*. (2019) 116:108999. doi: 10.1016/j.biopha.2019.108999

41. Kang J, Thakali KM, Jensen GS, Wu X. Phenolic acids of the two major blueberry species in the US market and their antioxidant and anti-inflammatory activities. *Plant Foods Hum Nutr*. (2015) 70:56–62. doi: 10.1007/s11130-014-0461-6

42. Mnich E, Bjarnholt N, Eudes A, Harholt J, Holland C, Jørgensen B, et al. Phenolic cross-links: building and de-constructing the plant cell wall. *Nat Prod Rep*. (2020) 37:919–61. doi: 10.1039/C9NP00028C

43. Reis B, Martins M, Barreto B, Milhazes N, Garrido EM, Silva P, et al. Structure–property–activity relationship of phenolic acids and derivatives. Protocatechuic acid alkyl esters. *J Agric Food Chem*. (2010) 58:6986–93. doi: 10.1021/jf100569j

44. Shin JU, Jo YH, Jeong SA, Jeong YH, Son MG, Jeong YJ, et al. Bioconverted blueberry extract potentiates the angiogenic and endothelial functions in human dermal microvascular endothelial cells under oxidative stress. *Curr Issues Mol Biol*. (2026) 48:224. doi: 10.3390/cimb48020224

45. Felgus-Lavefve L, Howard L, Adams SH, Baum JI. The effects of blueberry phytochemicals on cell models of inflammation and oxidative stress. *Adv Nutr*. (2022) 13:1279–309. doi: 10.1093/advances/nmab137

46. Duluc L, Jacques C, Soleti R, Iacobazzi F, Simard G, Andriantsitohaina R. Modulation of mitochondrial capacity and angiogenesis by red wine polyphenols *via* estrogen receptor, NADPH oxidase and nitric oxide synthase pathways. *Int J Biochem Cell Biol.* (2013) 45:783–91. doi: 10.1016/j.biocel.2013.01.007

47. Kuroyanagi G, Hioki T, Tachi J, Matsushima-Nishiwaki R, Iida H, Tokuda H, et al. Resveratrol inhibits basic fibroblast growth factor-induced macrophage colony-stimulating factor synthesis via the PI3-kinase/Akt pathway in osteoblasts. *Biosci Biotechnol Biochem*. (2023) 87:1462–9. doi: 10.1093/bbb/zbad121

48. Cerezo AB, Winterbone MS, Moyle CWA, Needs PW, Kroon PA. Molecular structure-function relationship of dietary polyphenols for inhibiting VEGF-induced VEGFR-2 activity. *Mol Nutr Food Res*. (2015) 59:2119–31. doi: 10.1002/mnfr.201500407

49. Cerezo AB, Gallardo-Fernandez M, Santana-Garrido Á, Hornedo-Ortega R, Vázquez CM, Troncoso AM, et al. Inhibition of ex vivo VEGF-induced angiogenesis by tyrosol and hydroxytyrosol: a quantitative three-dimensional mouse aortic ring model. *Food Funct*. (2025) 16:8594–603. doi: 10.1039/D5FO02820E

50. Pandey P, Lakhanpal S, Mahmood D, Baldaniya L, Kang HN, Hwang S, et al. Recent update of natural compounds as HIF-1α inhibitors in colorectal carcinoma. *Drug Des Devel Ther*. (2025) 19:2017–34. doi: 10.2147/DDDT.S511406

51. Latronico T, Rossano R, Miniero DV, Casalino E, Liuzzi GM. Neuroprotective effect of resveratrol against manganese-induced oxidative stress and matrix metalloproteinase-9 in an "in vivo" model of neurotoxicity. *Int J Mol Sci*. (2024) 25:2142. doi: 10.3390/ijms25042142

52. Ávila-Gálvez MÁ, Vico-Padilla A, Schneider C, Espín JC, González-Sarrías A, Giménez-Bastida JA. Angiogenesis as a therapeutic target of (poly)phenols: tackling cancer and vascular-related complications. *Mol Nutr Food Res*. (2025) 69:e70110. doi: 10.1002/mnfr.70110

53. Marrero AD, Cárdenas C, Castilla L, Ortega-Vidal J, Quesada AR, Martínez-Poveda B, et al. Antiangiogenic potential of an olive oil extract: insights from a proteomic study. *J Agric Food Chem*. (2024) 72:13023–38. doi: 10.1021/acs.jafc.3c08851

54. Baron-Menguy C, Bocquet A, Guihot AL, Chappard D, Amiot MJ, Andriantsitohaina R, et al. Effects of red wine polyphenols on postischemic neovascularization model in rats: low doses are proangiogenic, high doses anti-angiogenic. *FASEB J*. (2007) 21:3511–21. doi: 10.1096/fj.06-7782com

55. Martin S, Giannone G, Andriantsitohaina R, Carmen MM. Delphinidin, an active compound of red wine, inhibits endothelial cell apoptosis via nitric oxide pathway and regulation of calcium homeostasis. *Br J Pharmacol*. (2003) 139:1095–102. doi: 10.1038/sj.bjp.0705347

56. Oak MH, Bedoui JE, Madeira SVF, Chalupsky K, Schini-Kerth VB. Delphinidin and cyanidin inhibit PDGFAB-induced VEGF release in vascular smooth muscle cells by preventing activation of p38 MAPK and JNK. *Br J Pharmacol*. (2006) 149:283–90. doi: 10.1038/sj.bjp.0706843

57. Lamy S, Blanchette M, Michaud-Levesque J, Lafleur R, Durocher Y, Moghrabi A, et al. Delphinidin, a dietary anthocyanidin, inhibits vascular endothelial growth factor receptor-2 phosphorylation. *Carcinogenesis*. (2006) 27:989–96. doi: 10.1093/carcin/bgi279

58. Wang M, Feng J, Zhou D, Wang J. Bacterial lipopolysaccharide-induced endothelial activation and dysfunction: a new predictive and therapeutic paradigm for sepsis. *Eur J Med Res*. (2023) 28:339. doi: 10.1186/s40001-023-01301-5

59. Li H, Zhang Q. Research Progress of flavonoids regulating endothelial function. *Pharmaceuticals*. (2023) 16:1201. doi: 10.3390/ph16091201

60. Móritz AV, Horváth NL, Márton RA, Szilasi A, Jerzsele Á, Psáder R, et al. Anti-inflammatory effects of flavonoids in an LPS-induced in vitro model of canine chronic enteropathy. *Animals*. (2026) 16:450. doi: 10.3390/ani16030450

61. Sharma A, Lee HJ. Anti-inflammatory activity of bilberry (*Vaccinium myrtillus* L.). *Curr Issues Mol Biol*. (2022) 44:4570–83. doi: 10.3390/cimb44100313

62. Khan BV, Harrison DG, Olbrych MT, Alexander RW, Medford RM. Nitric oxide regulates vascular cell adhesion molecule 1 gene expression and redox-sensitive transcriptional events in human vascular endothelial cells. *Proc Natl Acad Sci*. (1996) 93:9114–9. doi: 10.1073/pnas.93.17.9114

63. Kim ME, Lee JS. Advances in the regulation of inflammatory mediators in nitric oxide synthase: implications for disease modulation and therapeutic approaches. *Int J Mol Sci*. (2025) 26:1204. doi: 10.3390/ijms26031204

64. Villarete LH, Remick DG. Nitric oxide regulation of IL-8 expression in human endothelial cells. *Biochem Biophys Res Commun*. (1995) 211:671–6. doi: 10.1006/bbrc.1995.1864

65. Zhou S, Yang L, Hu L, Qin W, Cao Y, Tang Z, et al. Blueberry extract alleviated lipopolysaccharide-induced inflammation responses in mice through activating the FXR/TGR5 signaling pathway and regulating gut microbiota. *J Sci Food Agric*. (2023) 103:4638–48. doi: 10.1002/jsfa.12560

66. Skrovankova S, Sumczynski D, Mlcek J, Jurikova T, Sochor J. Bioactive compounds and antioxidant activity in different types of berries. *Int J Mol Sci*. (2015) 16:24673–706. doi: 10.3390/ijms161024673

67. Del Bo C, Roursgaard M, Porrini M, Loft S, Møller P, Riso P. Different effects of anthocyanins and phenolic acids from wild blueberry (*Vaccinium angustifolium*) on monocytes adhesion to endothelial cells in a TNF-α stimulated proinflammatory environment. *Mol Nutr Food Res*. (2016) 60:2355–66. doi: 10.1002/mnfr.201600178

68. Song Y, Huang L, Yu J. Effects of blueberry anthocyanins on retinal oxidative stress and inflammation in diabetes through Nrf2/HO-1 signaling. *J Neuroimmunol*. (2016) 301:1–6. doi: 10.1016/j.jneuroim.2016.11.001

69. Auger C, Muzammel H, Diouf I, Schini-Kerth VB. Potential of anthocyanin-rich products to prevent and improve endothelial function and senescence: focus on Anthocyanins. *J Agric Food Chem*. (2024) 72:27590–618. doi: 10.1021/acs.jafc.4c04727

70. Mozos I, Flangea C, Vlad DC, Gug C, Mozos C, Stoian D, et al. Effects of Anthocyanins on vascular health. *Biomolecules*. (2021) 11:811. doi: 10.3390/biom11060811

71. Festa J, Da Boit M, Hussain A, Singh H. Potential benefits of berry Anthocyanins on vascular function. *Mol Nutr Food Res*. (2021) 65:e2100170. doi: 10.1002/mnfr.202100170

72. Ozorowski M, Wiciński M, Kuźmiński O, Wojciechowski P, Siedlecki Z, Śniegocki M, et al. The effects of quercetin on vascular endothelium, inflammation, cardiovascular disease and lipid metabolism—a review. *Nutrients*. (2025) 17:1579. doi: 10.3390/nu17091579

73. Vissenaekens H, Grootaert C, Raes K, De Munck J, Smagghe G, Boon N, et al. Quercetin mitigates endothelial activation in a novel intestinal-endothelial-monocyte/macrophage coculture setup. *Inflammation*. (2022) 45:1600–11. doi: 10.1007/s10753-022-01645-w

74. Ozyel B, Le Gall G, Needs PW, Kroon PA. Anti-inflammatory effects of quercetin on high-glucose and pro-inflammatory cytokine challenged vascular endothelial cell metabolism. *Mol Nutr Food Res*. (2021) 65:e2000777. doi: 10.1002/mnfr.202000777

75. Renny A, Sidhic J, Tom A, Kuttithodi AM, Job JT, Rajagopal R, et al. Methanol extract of *Thottea siliquosa* (lam.) ding Hou leaves inhibits carrageenan- and formalin-induced paw edema in mice. *Molecules*. (2024) 29:4800. doi: 10.3390/molecules29204800

76. Kulshreshtha S, Tandalekar YB, Goyal A, Srivastava AK, Jachak SM. Selected Indian medicinal plants exhibit anti-inflammatory activity by modulating pro-inflammatory cytokines *in vitro* and in carrageenan-induced rat paw edema. *Chem Biodiver*. (2025) 22:e03382. doi: 10.1002/cbdv.202403382

77. Meckes M, David-Rivera AD, Nava-Aguilar V, Jimenez A. Activity of some Mexican medicinal plant extracts on carrageenan-induced rat paw edema. *Phytomedicine*. (2004) 11:446–51. doi: 10.1016/j.phymed.2003.06.002

78. Gilligan JP, Lovato SJ, Erion MD, Jeng AY. Modulation of carrageenan-induced hind paw edema by substance P. *Inflammation*. (1994) 18:285–92. doi: 10.1007/BF01534269

79. Nardi GM, Farias Januario AG, Freire CG, Megiolaro F, Schneider K, Perazzoli MRA, et al. Anti-inflammatory activity of berry fruits in mice model of inflammation is based on oxidative stress modulation. *Pharm Res*. (2016) 8:S42–9. doi: 10.4103/0974-8490.178642